Post-curing process and visco-elasto-plastic behavior of two structural adhesives

Ignacio-Alberto Estrada-Royval, **Alberto Díaz-Díaz**

Abstract

The aim of this paper is to reveal original visco-elasto-plastic phenomena for two commercial epoxy adhesives (D609 and E20HP) subjected to uniaxial tension and compression. First, a post-curing heat treatment is proposed by means of thermal analyses in order to ensure stable mechanical properties. Bulk adhesive specimens are prepared to analyze the mechanical response of both materials. Monotonic tensile and compressive tests are carried out at different strain rates. Both adhesives exhibit first a linear elastic behavior but once a yield stress is reached, a visco-elasto-plastic behavior appears. Creep tensile tests are also carried out and confirm that strain rate phenomena take place and that non-negligible negative volumetric inelastic strains appear. Cyclic tests are also performed and reveal ratcheting effects. The applicability of the results to thin bondlines is discussed. The experimental observations must be taken into account in any model which aims at predicting accurately the behavior of the adhesives considered in this paper.

1. Introduccion

Adhesive joints represent great advantages over other assembly techniques and their applications are increasing every day. In order to optimize the design of this type of joints, it is important to know the adhesive behavior up to failure. Generally, this behavior is nonlinear because of phenomena such as plasticity [1],

damage [2] and visco-elasto-plasticity [3]. Several experimental and the-oretical studies focused on the non-linear behavior of polymers and adhesives have been published. Wang and Chalkley [4] carried out modified Iosipescu tests (multiaxial testing) with specimens of a commercial adhesive, and showed that a Drucker–Prager-type modified function adequately predicts yielding. By means of modified ARCAN tests, Cognard et al. [5] studied the elastoplastic behavior of another commercial epoxy adhesive at low tempera-tures to minimize the effects of viscosity. It was demonstrated that the hydrostatic stress has an effect on the non-linear behavior of the adhesive. On the other hand, it is worth stating that, for some adhesives, the loading rate may affect the mechanical response at room temperature [6]. For example, Pap et al. [3] tested under tension and compression, a commercial adhesive, put in evidence a strain rate-dependent behavior, and used a linear viscoelastic model which failed to correctly predict the behavior because it did not include plasticity. In [7], Cognard et al. tested another commercial epoxy adhesive at room temperature by means of modified ARCAN cyclic tests, and at different rates. It was demonstrated that the behavior of the studied adhesive was visco-elasto-plastic.

The visco-elasto-plastic behavior of polymers has been widely studied but a general 3D model validated by 3D tests has not been yet developed. This is surely due to a lack of experimental data. Drozdov has developed 1D visco-elasto-plastic models based on uniaxial tensile tests and which predict accurately axial strains and stresses for several polymers [8–11]. Mahnken et al. developed a 3D visco-plastic model for a glassy polymer and compared its predictions to the axial strains and

stresses in uniaxial tensile and compressive monotonic tests carried out at different strain rates [12]. This model reproduced well the experimental asymmetry: maximum stresses in compression were higher than those in tension. Chaboche [13] and Poulain et al. [14] also developed 3D viscoplastic models but only confronted their predictions to the axial strains and stresses in uniaxial tensile and compressive monotonic tests. In fact, the measurement of the transverse strains is seldom reported and without it, a full description of the strain state cannot be achieved. This measurement not only provides a Poisson's ratio but also valuable information about inelastic volu-metric strain rates which may help, for example, to test the accuracy of a von Mises-type yield criterion that predicts, in the case of associative plasticity, a zero volumetric strain rate [15].

It is important to note that the mechanical characterization of a thermosetting adhesive cannot ignore a thermal study of the adhesive and its curing. Remaining chemical reactions may occur after curing and the mechanical properties may vary with time and temperature [16]. A post-curing heat treatment at a moderate temperature above the glass transition temperature (Tg) may help to achieve the thermal stability of the polymer [17]. Care must be taken in the selection of the post-curing temperature because if it is too high, it may cause a degradation of the mechanical prop-erties of the polymer [16, 18]. Several authors suggest and apply a post-curing heat treatment to adhesives in structural assemblies and resins in dental applications to ensure stable mechanical properties and to improve them [19–21]. For example, Cognard et al. [22] proposed a post-curing process of 50 °C during 4 h for aluminum adhesive joints using an epoxy adhesive (Vantico Redux 420). In spite

of the publications involving post-curing heat treatments to adhesives, little or no information of the procedure adopted to select the temperature and duration of the treatment is provided.

In this document, the mechanical response of two commercial epoxy adhesives is studied. Uniaxial tensile and compressive tests are performed at room temperature. A post-curing heat treatment is developed and proposed to achieve stable mechanical proper-ties. The effect of the temperature reached during curing on the properties of the adhesives and the applicability of the experi-ments in this paper to adhesive joints are discussed. The mechanical tests performed are monotonic at different strain rates, of creep- and cyclic-type. Axial and transverse strains are measured to provide a full description of the strain state in the spe-cimens. In the mechanical tests, visco-elasto-plastic phenomena which have not been reported previously for thermosetting polymers are put in evidence. For example, the volumetric inelastic strains are non-negligible and volumetric strains may be negative in tensile tests. Negative volumetric strains in uniaxial tension have not been reported for epoxy polymers [23], but only for thermoplastic polymers such as polyvinylidene fluoride in large strains in a rubbery state [24,25] and polycarbonate in a glassy state [26]. Taking into account the experimental observations, recommendations are made for future models aimed at predicting correctly the mechanical behavior of epoxy adhesives.

In this article, the materials and methods used are presented first. The results are provided later. Then, a discussion of these results is presented with an emphasis on the new elements pro-vided by the research presented herein. The conclusions

of this work are presented at the end of the document.

2. Materials and methods

2.1. Materials

The epoxy adhesives studied are D609 and E20HP, both fast curing two-component structural adhesives from Hysol line by Henkel. These adhesives are recommended to be used with metals, polyester, glass, wood, etc. The manufacturer recommends a curing temperature of 25 °C for 24 h for both adhesives. D609 is recommended for applications at low temperatures and, as for E20HP, there is no recommendation on the working temperatures in the specifications but a graph is provided, showing that the strength of an adhesive joint with aluminum decreases as the temperature increases from 25 °C, approximately. The Tg is only provided for E20HP: 60 °C.

The manufacturer indicates that the D609's resin is composed of epichlorohydrin-4, 4′-isopropylidene diphenol, while the E20HP's resin contains acrylic polymers. The D609's hardener consists of a polymercaptan and a tertiary amine. The E20HP's hardener consists of polyamine, polyglycol diamine, salicylic acid, glycerol, aminophenol, diethyleneglycol monoethyl ether and ethylene glycol. Each two-component adhesive is contained in a cartridge. A mixing nozzle is used with the cartridge to apply the mixture of resin and hardener. The mechanical properties of adhesives depend on the curing condition and degree. According to the manufacturer, both adhesives (D609 and E20HP) have a maximum strength after having cured for 24 h at 25 °C. However, there is no guarantee whatsoever that under these conditions, all reactions will be completed and that the mechanical

properties will remain stable after being subjected to temperature variations [16]. In this sense, in this work, the choice has been made to determine a post-cure heat treatment. It would have been possible to think of a curing at a higher temperature, but this method was discarded because of the advantage of handling and curing an adhesive within an adhesive joint at room temperature.

2.2. Post-curing heat treatment

This treatment is aimed at stimulating the remaining reactions within the adhesive specimens cured at room temperature in order to achieve a nearly complete curing and stable mechanical properties. This section describes the procedures to determine the temperature and post-curing time for adhesives cured at 25 °C for 24 h.

For each adhesive, we began by carrying out a thermogravi-metric analysis (TGA) of the resin, the hardener and the cured adhesive so as to verify that the constituents do not experiment degradation and determine up to which temperature level it is possible to execute the post-cure treatments without degrading the adhesive. One repetition was considered and the heating rate employed was 10 °C/min. Later on, in a differential scanning calorimeter (DSC), analyzing the heat power per unit mass, the adhesives were monitored at 25 °C, to verify the curing time proposed by the manufacturer (one repetition per adhesive was performed). Then, on the same device, a temperature scanning was performed with cured samples in order to verify that there are remaining exothermic reactions. Subsequently, in the DSC, cured samples were subjected to constant temperatures (50 °C, 60 °C, 70 °C, 80 °C, 90 °C, and 100 °C) to select the time and temperature

for the post-curing treatment. Finally, the post-cured samples were subjected to a temperature scanning in the same device in order to verify that, virtually, there is no remaining reaction that may be stimulated by a temperature increase. This temperature scanning also made possible to make a first estimation of Tg. It is worth stating that temperature scannings in the DSC were made at a heating rate of 5 °C/min from -50 °C upto140°C.

A second estimation of Tg was provided by a dynamical mechanical analysis (DMA) and a temperature scanning. The samples intended for this technique were obtained by pouring the adhesive in urethane molds at room temperature and, after the curing, a heat treatment was applied with the parameters deter-mined by the DSC. Afterwards, the faces were rectified in a milling machine to obtain specimens which are 12 mm wide, 3 mm thick, and 50 mm long. A three point flexural test was carried out with a 44 mm span length. The test frequency and amplitude were 1 Hz and 4.5 N, respectively. A 6 N-preload was used to ensure that the specimen was always in contact with the supports. The dimensions and applied loads yield a 6.41 MPa maximum flexural stress which, at room temperature, does not cause plastic strains in quasi-static monotonic tests (see Section 3.2). The temperature range was from -30 °Cto100 °C at a heating rate of 5 °C/min. One test per adhesive was carried out.

2.3. Uniaxial mechanical testing

Uniaxial tension and compression tests were performed in an electromechanical machine Instron 3382 to study the mechanical behavior of the adhesives and analyze a potential asymmetry. In all cases, strain gage rosettes

(containing three strain gages, with the second and third gages angularly displaced from the first gage by 45° and 90°, respectively) were used to measure accurately the principal strains (axial and transverse strains) avoiding any sensitivity to a misalignment of the rosette with respect to the axial direction. The tests were performed at a constant temperature of 25 °C and the relative humidity of air was 20%.

In order to make adhesive specimens for these mechanical tests, Teflon molds were built to cast the mixture before the curing (see Fig. 1). After curing for 24 h at 25 °C, the samples were extracted from the mold to be subjected to a heat treatment at 70 °C for 2 h (heating and cooling were carried out at 7 °C/min and -1°C/min). The specimens section for tensile tests is circular with larger diameter at the ends where the jaws fasten the sample, and in the central zone, it has a 7 mm diameter and a 44 mm length. The specimens for compression test were extracted from untested tension specimens and have a 7 mm diameter and a 16 mm length. The faces of the specimens were rectified in a lathe. In Fig.1, the picture of D609 specimens for tensile and compressive tests are shown. The strain gage rosettes used for the strain measurement are shown as well.

The mechanical tests carried out for each adhesive were as follows:

- Monotonic compressive and tensile tests. The applied strain rates were 12%/min, 2%/min, and 0.2%/min.
- Creep tests. The tests consisted in reaching a certain load level at a constant rate (300 MPa/min), and then maintaining that load level until the failure occurs. The loads used for D609 were 30, 32.5, 35, 37.5,

and 40 MPa, and for E20HP 25, 27.5, 30, 32.5, and 35 MPa. These load values were selected after an analysis of the results of monotonic tests. These creep tests are typical for analyzing visco-elasto-plastic behaviors. Additionally, a multicreep tensile test was carried out for each adhesive. In this test, successive 2.5 MPa load increments at a 300 MPa/min rate were followed by a 10 min stress plateau. This multicreep test provides usually complementary information for the analysis of a time dependent behavior

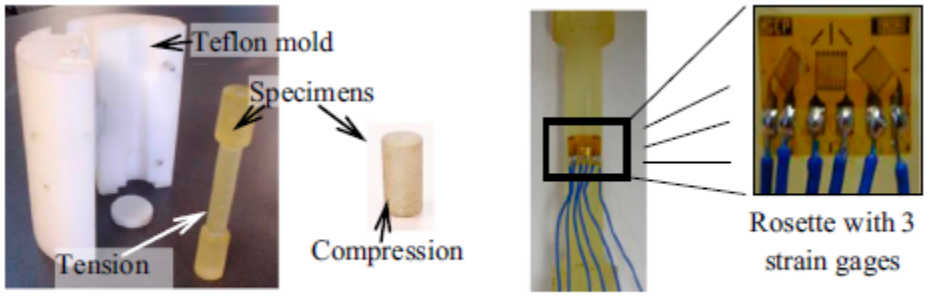

Fig. 1. Specimens obtained from Teflon molds for tensile and compressive tests.

- Loading and unloading test. This type pf test consisted in applying compressive stress progressively up to a certain level (25 MPa for both adhesives), and subsequently downloading until getting to zero stress and observing the specimen recovery by monitoring the strain. This determines if there is plasticity or the material. Both the loading and the unloading rates were 0.2%/min.
- Cyclic test. These test were performed both for tension and compression at a 2%/min strain rate. The maximum loads were 30 MPa and 25 MPa for D609 in tension and compression, respectively.

For the E20HP adhesive, the maximum load was 25 MPa in tension and compression. With these test, it is possible to put in evidence phenomena such as ratcheting and accommodation.

3. Results

3.1. Post-curing treatment selection

The TGA made possible to determine the temperature range for selecting the post-curing treatment without degrading the material. In Fig. 2a and b, it is possible to appreciate that, at temperatures above 200 °C, there is a remarkable mass decrease of previously cured adhesives. At 100 °C, mass losses are less than 0.35% for both adhesives, these losses are surely due to evaporation of water absorbed by the polymers. If the temperature of 100 °C is selected as the maximum usable temperature in the post-curing treatment, no degradation of the cured adhesives would occur. For the resin and catalyst of each adhesive, a TGA analysis was also carried out, and it was noted that there is no degradation of the materials at temperatures below 30 °C (mass losses are less than 0.02%, see Fig. 2a and b). Thus, when the adhesive mixture is cast in the molds at 25 °C, negligible mass loss and degradation Is expected.

In the DSC device, the adhesives curing at 25 °C was monitored and the heat flow was plotted against time in Fig. 3 (one repetition was performed for each adhesive). It may be appreciated that, the curing reaction is exothermic for both adhesives and, that after 2 h, the heat released by exothermic phenomena is negligible for D609. For E20HP, the exothermic process lasts 5 h (not shown in the figure). Nevertheless, a 24-h curing is recommended by the manufacturer to ensure

that, from a mechanical standpoint, the adhesives achieve their optimal properties. It is worth mentioning that in all the graphs corresponding to a DSC test, the weight of

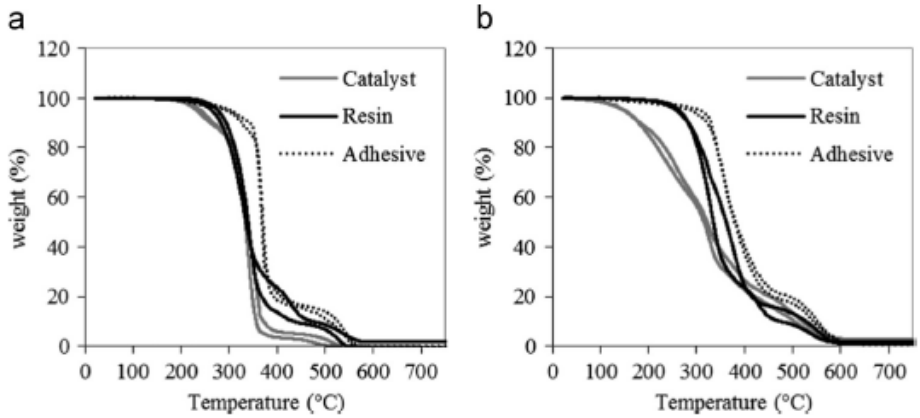

Fig. 2. TGA results for D609 (a) and E20HP (b) with one repetition per case.

The sample is indicated in the legend of the figure. The temperature scanning for both cured adhesives gave the graphs in Fig. 4. We may see after a slight decrease an abrupt drop around 25 °C and 35 °C for D609 and E20HP, respectively, most probably due to the material softening. Afterwards, an important increase in heat power is registered around 37 °C and 45 °C for D609 and E20HP, respectively, which puts in evidence remaining exothermic phenomena surely due to cross-linking reactions in both adhesives. Later, a significant exothermic peak for D609 at 95 °C and a smooth exothermic peak for E20HP at 110 °C are observed. These peaks may be caused by the remaining cross-linking reactions (non-instantaneous) which may be more exothermic for D609 than those for E20HP (in a similar magnitude order as that for the exothermic peaks during the curing process at 25 °C shown in

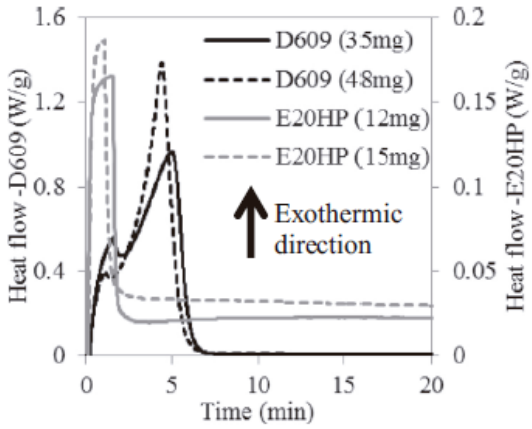

Fig. 3. Heat flow vs. time curves during the curing process at 25 °C of adhesives (DSC).

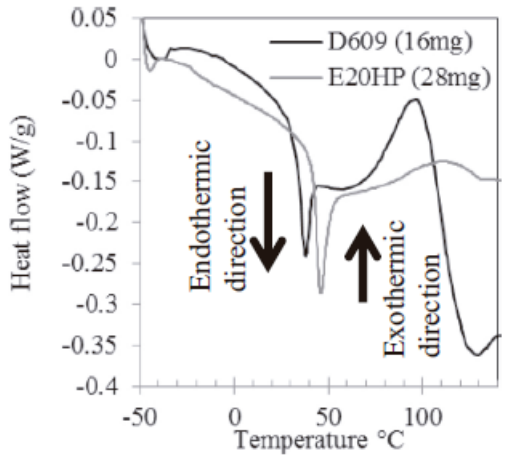

Fig. 4. DSC heating scan of adhesive specimens cured at 25 °C.

Fig. 3). The post-curing temperatures were thus selected greater than 50 °C so as to promote the remaining reactions.

Isothermic tests at 50, 60, 70, 80, 90 and 100 °C in the DSC with samples previously cured at 25 °C allowed obtaining the graphs in Fig. 5 for D609 and 6 for E20HP. In these tests, the heat flow was monitored only during 20 min because it was virtually zero after this time. We can see once again the presence of exothermic phenomena whose duration depends on temperature and the type of adhesive Fig.

6. After a 2-h heat treatment, samples were subjected to a temperature scanning in the DSC and the graphs in Figs. 7 and 8 were obtained for D609 and E20HP, respectively. It is possible to appreciate that the heat treatment at a lower temperature which does not show significant exothermic events is the one carried out at 70 °C. For this reason a post-curing process at 70 °C was selected for 2 h (longer than the duration of exothermic phenomena to ensure that no more exothermic reactions occur). Furthermore, as shown in Figs. 7 and 8, in the temperature scanning curve of adhesives post-cured at 70 °C, we may see that beyond 40 °C a decrease in the heat flow (endothermic phenomenon) most probably due to a material softening. Tg lies approximately between 40 °C and 60 °C for both adhesives post-cured at 70 °C. A better estimation of Tg is provided by the DMA tests.

By means of the temperature scanning tests with the DMA, the evolutions of the storage modulus E' and of tan (δ) against temperature were obtained for D609 (see Fig. 9a) and E20HP (see Fig. 9b) adhesive specimens post-cured with the selected process. δ is the phase angle difference between the displacement and the force applied by the machine. For the considered load amplitudes and 1 Hz frequency, tan(δ) increases considerably from 20 °C and 35 °C for D609 and E20HP, respectively. Above these temperatures, viscous phenomena are expected. Tg is estimated by the temperature at which the maximum value of tan(δ) is reached. For D609 and E20HP Tg'sare 45°C and 59 °C, respectively.

3.2. Monotonic tests

For both adhesives, Fig. 10a and b shows the stress–strain curves in

monotonic tensile and compressive tests at different loading rates, respectively. For sake of simplicity, the absolute values of strains and stresses are applied in Fig. 10b. It is clear that, at the beginning of the test, there is a linear zone virtually independent of the strain rate. Young's moduli calculated by the initial slopes of the curves in Fig. 10a and b are shown in Table 1. For each specimen, once the stress exceeds a yield value (greater than 20 MPa and 10 MPa for D609 and E20HP, respectively), a non-linear behavior which depends on the loading rate is exhibited. At this point, we can say that for strain rates lower than 12%/min, there is no significant viscoelastic phenomenon when the stress is lower than the above values. At first sight, this may seem

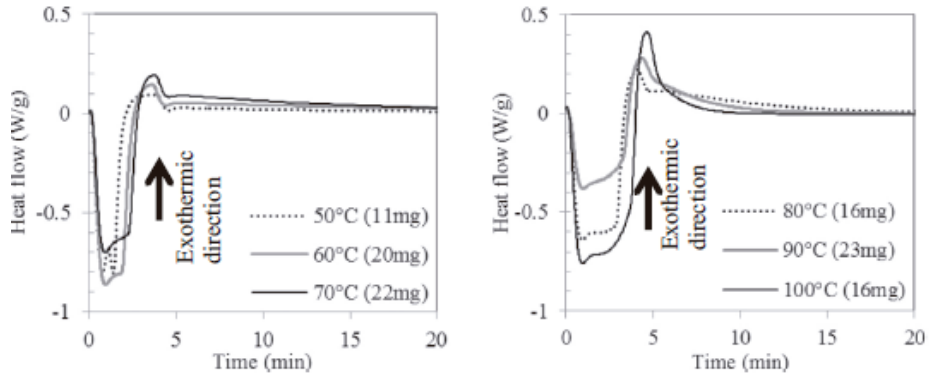

Fig. 5. Isothermal DSC curves for D609 post-cured at 50, 60, 70, 80, 90 and 100 °C.

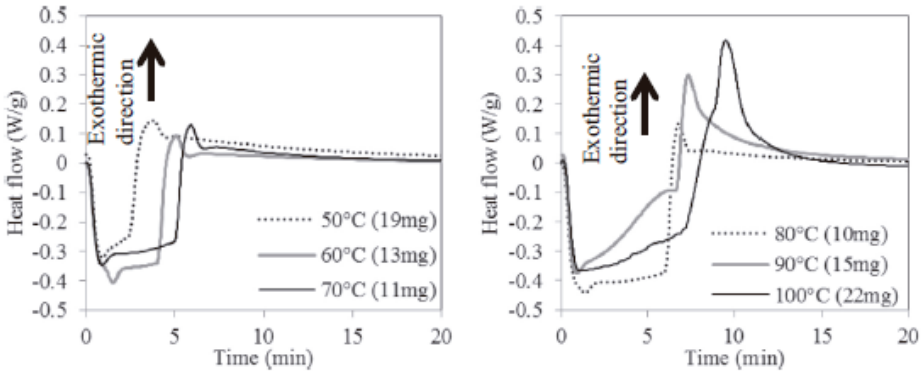

Fig. 6. Isothermal DSC curves for E20HP post-cured at 50, 60, 70, 80, 90 and 100 °C.

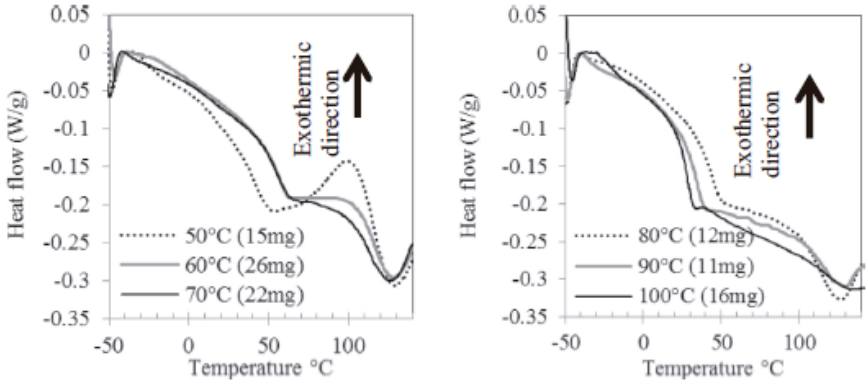

Fig. 7. DSC heating scan of D609 post-cured at 50, 60, 70, 80 90 and 100 °C.

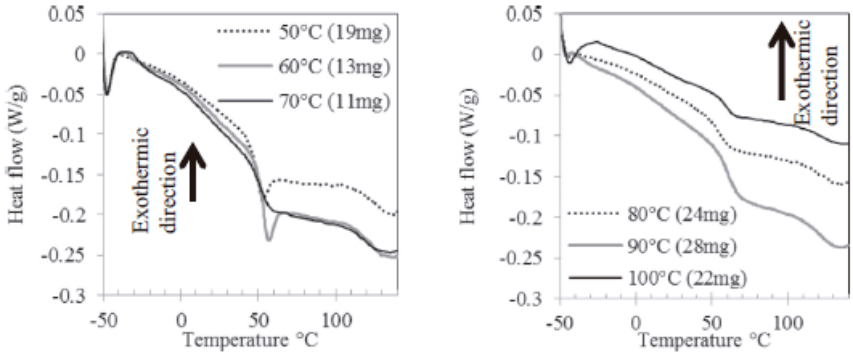

Fig. 8. DSC heating scan of E20HP post-cured at 50, 60, 70, 80 90 and 100 °C.

Contradictory with what has been said for D609 in the DMA test in the previous section: above 20 °C viscous phenomena are expected because tan(δ) increased considerably from this temperature. Nevertheless, this has been said for a loading rate of 1 Hz which causes a much higher strain rate than 12%/min. The cyclical tests, which will be later presented, show that there are plastic strains and, therefore, the non-linearity in the monotonic tests is due to a visco-elasto-plastic phenomenon. For both adhesives, the maximum stresses exhibit an asymmetry: the maximum stresses reached in compression are greater than those in tension.

In the monotonic tests, transverse strains were also measured. Poisson's

ratios measured in these tests are listed in Table 1. The volumetric strains εva=+x2εεt were deduced from the axial strain εax and transverse strain εt and were plotted against the axial strains in Fig. 11a and b in tension and compression, respectively.

Let us indicate that in these figures, the real algebraic values of the axial strain and volumetric strains were considered (no change in sign was made). Once again, for small strains, a linear elastic behavior which does not depend on the strain rate is observed and is followed by a strain rate dependent, non-linear behavior. For both adhesives in tension and in compression, during the linear stage, the volumetric and axial strains have a same sign and vary proportionally. For the non-linear stage, there is not a simple qualitative rule to predict how the shape of the curves varies as the strain strain rate increases. In spite of this, it is clear that during the non-linear stage, significant inelastic volumetric strains provoke a change in sign in the derivative of the volumetric strain vs axial strain curves. The magnitude of these inelastic volumetric strains is such that for some E20HP specimens and all D609

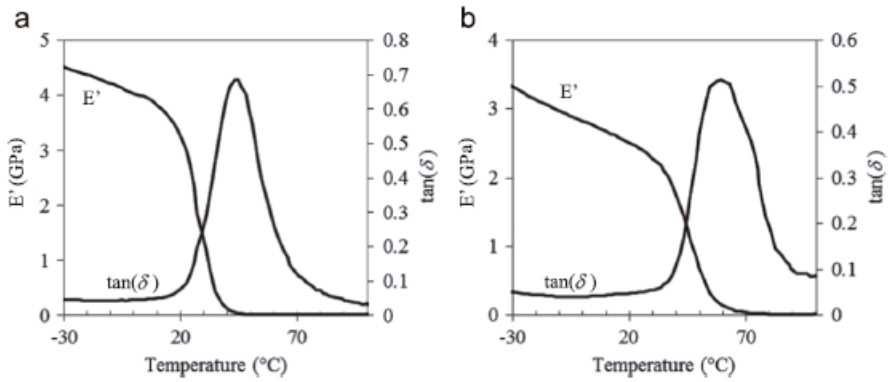

Fig. 9. DMA temperature scanning for D609 (a) and E20HP (b).

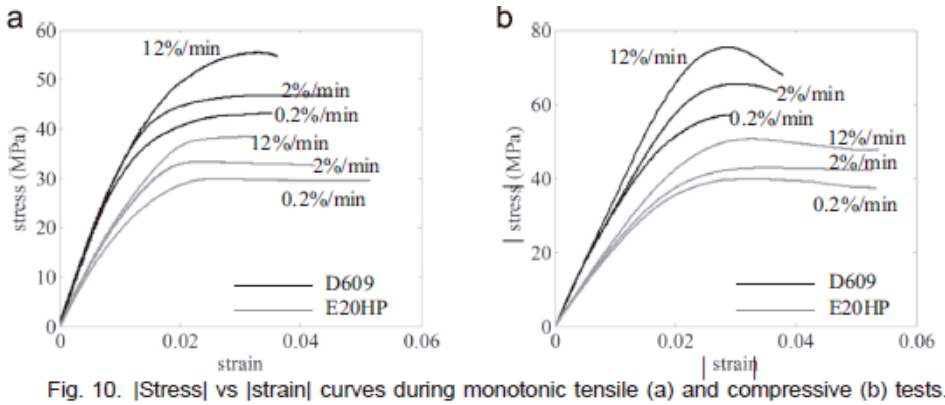

Fig. 10. |Stress| vs |strain| curves during monotonic tensile (a) and compressive (b) tests.

Specimens in tension (compression), negative (positive) volu-metric strains appear. The fact that the shape of the curves does not vary monotonically as the strain rate increases may be due to a competition of viscoelastic and viscoplastic phenomena. The densification in tension and global expansion in compression may seem surprising and “anomalous”. In Section 4.2, the accuracy of the deduction of the volumetric strains and the possible reasons of the “anomalous” values of the volumetric strains are discussed.

3.3. Creep tests

For the creep testing under tension, the total strain evolution as a function of time for the two adhesives was graphed in Fig. 12.In these tests, a fast monotonic load until reaching the desired stress level was applied. Under constant stress, the elastic strain is constant and the total strain variation is due to a variation of inelastic strains. We can see in this figure that the higher the load level, the higher the rate is at which viscous strains increase with respect to time. It is also possible to appreciate that, from a curve under a certain load level, it is not possible to deduce the other one by a simple factor of proportionality between load levels; therefore, the

behavior is not linear viscoelastic. After the creep stress is maintained, the strain rate is virtually constant and depends on the stress level.

In the same way, for these tests, the volumetric strain evolution was plotted as a function of time (see Fig. 13). For both adhesives, except for the test at 30 MPa with D609, we can observe a volumetric strain decrease. Once again as in monotonic tensile tests, a densification is observed. The volumetric strain variations cannot be disregarded with respect to the axial strain since they reach values greater than 20% of the axial strains. For the 30 MPa test on

Table 1
Young's modulus (E) and Poisson's ratios (ν) in tension and compression at different strain rates.

Adhesive		Tension			Compression		
		0.2%/min	2%/min	12%/min	0.2%/min	2%/min	12%/min
D609	E (GPa)	3.42	3.11	3.31	3.51	3.55	3.38
	ν	0.39	0.41	0.38	0.41	0.43	0.41
E20HP	E (GPa)	2.25	2.49	2.51	2.11	2.06	2.39
	ν	0.40	0.39	0.39	0.41	0.39	0.40

D609, the volumetric strain remains positive. In the other tests the volumetric strain becomes negative and its magnitude increases with time. Except for the 32.5 MPa or the 35 MPa creep test on D609, as the stress level increases the magnitude of the volumetric strain rate increases. This exception may be due to experimental dispersion or a competition between viscoelastic and viscoplastic phenomena.

The tensile multicreep tests confirmed that the behavior is not linear viscoelastic. In Fig. 14a and b, the axial strain was plotted against time for D609 and E20HP, respectively. Let us recall that successive 2.5 MPa stress increments were applied after a 10 min constant stress hold. During each constant stress stage, the

strains increase with time but this increase depends on the stress level. The greater the stress level, the greater the strain increase.

3.4. Results of cyclic tests

Fig. 15a and b shows the stress–strain graphs from the cyclic tensile tests for D609 and E20HP, respectively. A ratcheting

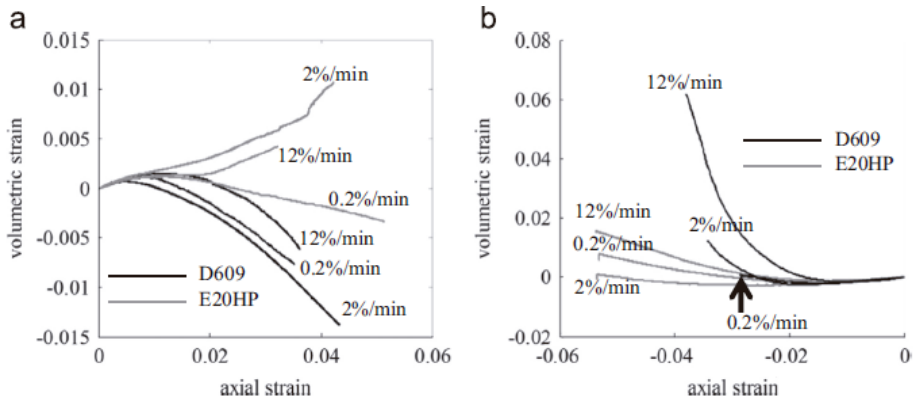

Fig. 11. Volumetric strain vs axial strain curves during monotonic tensile (a) and compressive (b) tests.

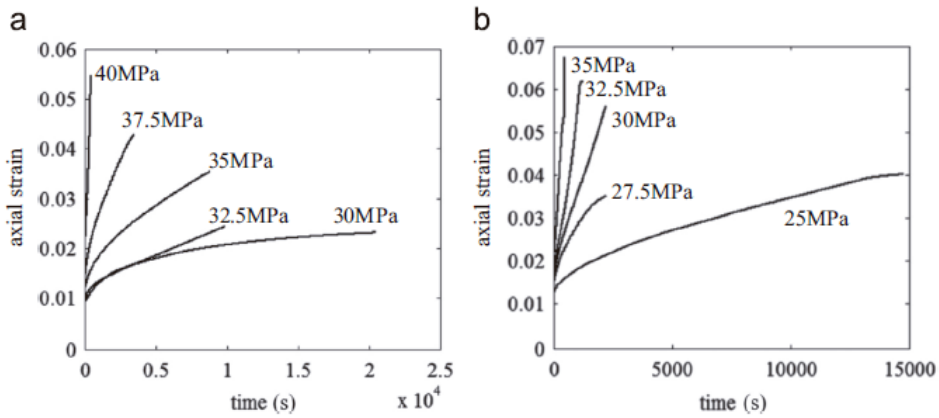

Fig. 12. Axial strain vs time curves for D609 (a) and E20HP (b) during tensile creep tests.

Phenomenon is observed for both adhesives. One may observe hysteresis loops and one would expect a Bauschinger effect if the unloading was carried out up to negative stresses. In Fig. 16a and b, the stress–strain graphs from the cyclic compressive tests for D609 and E20HP are shown, respectively. For sake of

simplicity, the absolute values of strains and stresses are applied in these figures. Analog comments as those for tension can be added. Fig. 17a and b shows the evolution of the ratcheting strain against the number of cycles for D609 and E20HP, respectively. After 30 cycles, the ratcheting strain is non-zero and the accommodation phenomenon does not take place.

For the loading and unloading tests under compression (a single cycle), stress was graphed against strain for both adhesives in Fig. 18a. The axial strain evolution against time was graphed in Fig. 18b. In this figure, a horizontal asymptotic evolution is appreciated for the zero stress stage, which implies a permanent plastic strain. This proves that viscoelasticity alone is not able to predict the observed phenomena.

4. Discussion

4.1. Stability of the properties of post-cured specimens

The post-curing heat treatment selected allowed to promote remaining reactions, and according to the temperature scanning in the DSC, there are no more significant remaining exothermic reactions. To confirm that the mechanical properties remain stable after the post-curing treatment, a post-cured specimen of each adhesive was subjected to a temperature scanning in the DMA from -30 °Cupto0°C, then it was introduced in an oven at a temperature of 70 °C for 2 h to simulate an exposition to a higher temperature, and finally it was subjected to a temperature scanning in the DMA from -30 °Cupto100°C. Fig. 19 shows the plot of the storage modulus against temperature for the sample before and after being exposed to a higher temperature. For both adhesives, it is possible to observe that

virtually the same curves are obtained before and after the exposition to a higher temperature, which demonstrates that the mechanical properties are stable.

It is worth saying that in the temperature scannings in the DMA referred in the above paragraph, the specimens before the temperature exposition were not subjected to a higher temperature because, otherwise, with the material being subjected to mechanical loads and temperatures above the softening temperature, plastic strains in the specimens may appear, so that it would not be possible to reuse them for a new test in the DMA. After the temperature scannings below 0 °C, the specimens were inspected. It was observed that they kept the same geometry and, therefore, there were no plastic strains. In fact, the dimensions and applied load provided in Section 2.2 yield a 6.41 MPa maximum flexural stress and according to the results obtained in Section 3.2 for monotonic tests, this stress level is not enough to make appear plasticity at room temperature. At higher temperatures, plasticity may occur because the yield stress decreases with increasing temperature.

4.2. Densification in tension and expansion in compression: a result of inaccurate measurements or an authentic phenomenon?

In Sections 3.2 and 3.3, negative (positive) volumetric strains were determined in certain stages of most tensile (compressive)

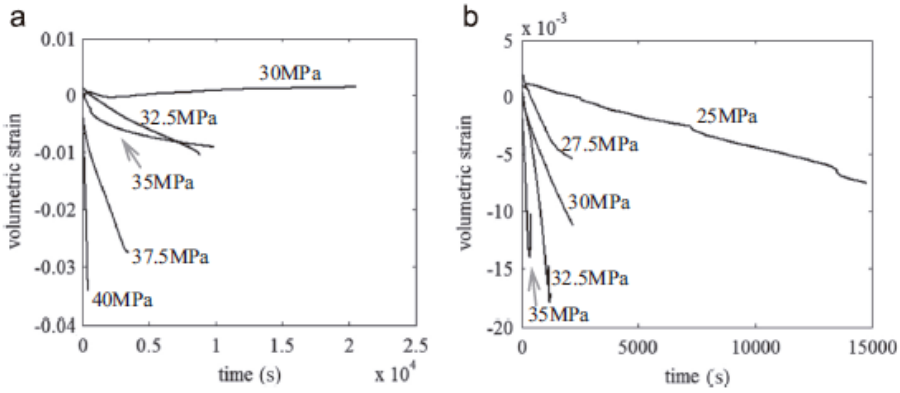

Fig. 13. Volumetric strain vs time for D609 (a) and E20HP (b) during tensile creep tests.

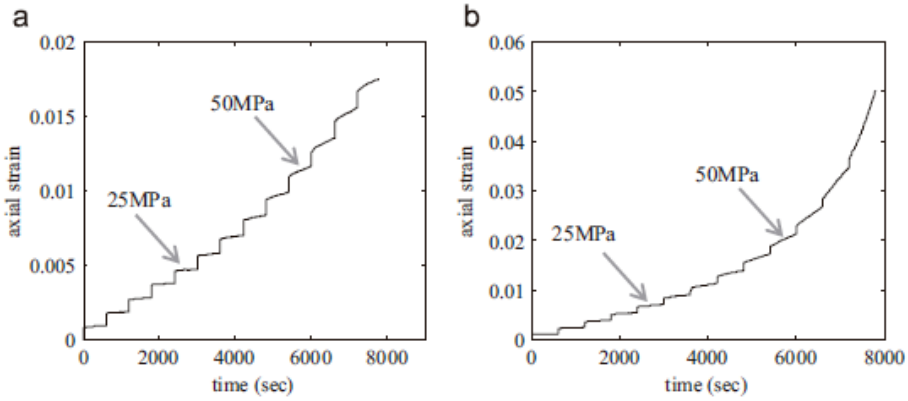

Fig. 14. Axial strain vs time for D609 (a) and E20HP (b) during tensile multicreep tests.

Tests. The volumetric strains εva=+x2εεt were deduced from the axial and transverse strains: εax and εt , respectively. εax and εt were determined by making use of strain gage rosettes and a National Instruments Data Acquisition System. Let us make an analysis of the reliability of the values of the volumetric strains. The possible error in the measurement of a strain is considered (not greater than Δε =0.4% and caused by the variability in the gage factor and resistance of the strain gage and wires). Let us recall that the measurement of the in-plane principal strains is insensitive to a misalignment of the rosette with respect to the axial direction (in our uniaxial tests, the principal strains are the axial and transverse strains).

In tension, the measured axial strain εax and the exact axial strain εax0 are positive, whereas the measured transverse strain εt and the exact transverse strain εt0 are negative; thus

$$\varepsilon_{ax}^{0} \times (1 - \Delta\varepsilon) \leq \varepsilon_{ax} \leq \varepsilon_{ax}^{0} \times (1 + \Delta\varepsilon)$$

$$\varepsilon_{t}^{0} \times (1 + \Delta\varepsilon) \leq \varepsilon_{t} \leq \varepsilon_{t}^{0} \times (1 - \Delta\varepsilon)$$

If the exact volumetric strain εv0 is non-zero, the deduced volumetric strain εv is related to εv0 as follows:

$$\varepsilon_{v}^{0} - \eta\left|\varepsilon_{v}^{0}\right| \leq \varepsilon_{v} \leq \varepsilon_{v}^{0} + \eta\left|\varepsilon_{v}^{0}\right|$$

Where η is the maximum relative error (η > 0) defined by

$$\eta = \frac{\left(\varepsilon_{ax}^{0} - 2\varepsilon_{t}^{0}\right)\Delta\varepsilon}{\left|\varepsilon_{v}^{0}\right|} = \frac{2\varepsilon_{ax}^{0} - \varepsilon_{v}^{0}}{\left|\varepsilon_{v}^{0}\right|}\Delta\varepsilon$$

Let us analyze the case where ηε>Δ . Then, the values of εv0 and

εax0 for which the maximum relative error is η (for example 0.1) are related by

$$\varepsilon_{v}^{0} = \frac{2\Delta\varepsilon}{\Delta\varepsilon + \eta}\varepsilon_{ax}^{0} \quad \text{and} \quad \varepsilon_{v}^{0} = \frac{2\Delta\varepsilon}{\Delta\varepsilon - \eta}\varepsilon_{ax}^{0}.$$

The relations above are valid for the compression case as well. These equations define two lines in a volumetric vs axial strain plot. In Fig. 20a and b, for η =0.1 in red and η =0.01 in green, these lines were added to the volumetric vs axial strain graphs obtained in monotonic tensile and compressive tests (displayed in Fig. 11a and b), respectively. Therefore, the percentage uncertainty in the calculation of volumetric strains for points which fall in region

- I (between the red lines) is greater than 10%
- II (between the red and green lines) is less than 10% but greater than 1%
- III (outside the region delimited by the green lines) is less than 1%.

In this manner, we confirm that in some E20HP and D609 specimens in monotonic tension (compression), negative (positive) volumetric strains appear. A similar analysis for the creep tensile tests has been carried out and proved that in all tests with both specimens, the percentage uncertainty in the calculation of volumetric strains is less than 10%. The “anomalous” densification in tension and expansion in compression are confirmed, they are not a result of small errors in the measurement of strains.

Let us now discuss about the originality of these results and provide a possible explanation to these “anomalous” phenomena. In

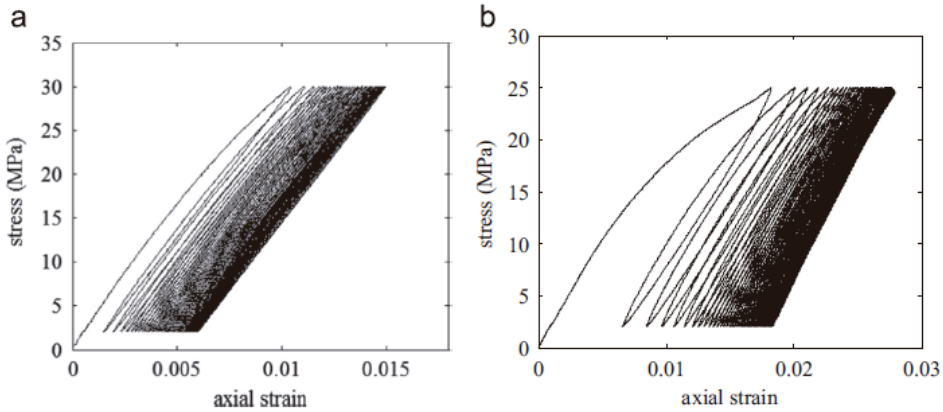

Fig. 15. Stress vs strain curves for D609 (a) and E20HP (b) during cyclic tensile tests.

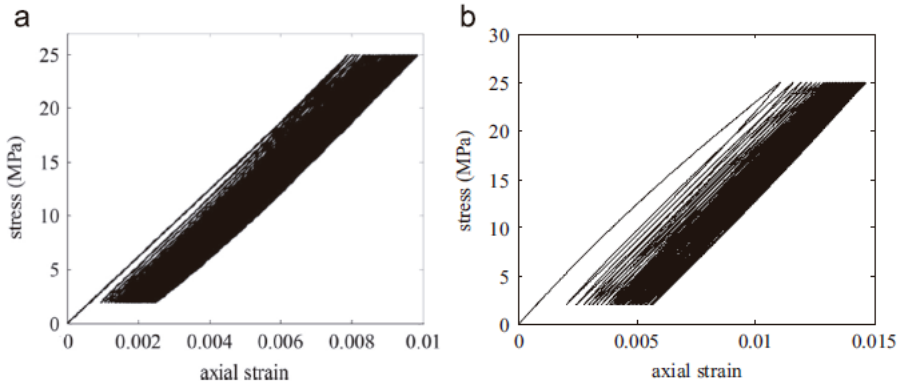

Fig. 16. |Stress| vs |strain| curves for D609 (a) and E20HP (b) during cyclic compressive tests.

tension, negative volumetric strains have not been reported for epoxy polymers, but only for some thermoplastic polymers tested in a rubbery state [24,25] and in a glassy state [26].In [24,25], thisdensification was justified by a possible orientation or alignment of chain segments in the amorphous material. Colucci et al. [26] argued that this densification is consistent with the “accelerated” aging hypothesis of Myers et al. [27]. Physical aging is characterized as an increase in mass density (specific volume decrease) and/or a decrease in molecular configurational energy (enthalpy relaxation) of amorphous materials when exposed to temperatures below Tg for extended periods of time [23]. Physical aging can be erased by heating the polymer above Tg during a certain period of time and cooling it to the original temperature; in this process, the specific volume increases. Oyanguren et al. claimed that a “mechanical rejuvenation” might occur when post-yield compressive stresses are applied [28].This was deduced by making a DSC temperature scanning with samples of two epoxy polymers and observing that, the response of aged samples that were subjected to a 28% compressive axial strain is similar to that of fresh thermally rejuvenated samples and very different from that of

aged ones which were not subjected to any mechanical load. In this sense, the positive volumetric strains measured in compression in the present paper are consistent with the hypothesis of “mechanical rejuvenation”. To our knowledge, positive volumetric strains in compression have not been previously reported for any epoxy polymer.

The densification in tension and expansion in compression reported in this paper may be interpreted as “mechanical accelerated aging” and “mechanical rejuvenation”, respectively. Nevertheless, the measurement of the specific volume is not enough to evaluate aging or rejuvenation in glassy polymers. In fact, there is a debate over the similarity of “mechanical rejuvenation” and thermal rejuvenation [23,29]: are the properties of a mechanically rejuvenated polymer the same as those of a thermally rejuvenated one? One may ask the same question for mechanical and physical aging. A more acceptable interpretation of the “anomalous” volumetric strains after yielding reported herein is a transition from an amorphous phase to another amorphous one which yields a different specific volume. This idea of phase transition was originally speculated by McKenna [29] to give an alternative explanation different from “mechanical rejuvenation” at post-yield applied loads and was reinforced by the molecular simulations of Lacks and Osborne in [30] who proved that shear loads may lead to a state that resembles the less-aged states but that is not identical to them. Further research is needed to justify these interpretations.

4.3. Relevance to adhesive joints

If one considers a steel adhesive joint with a thin adhesive layer, it is natural

to assume that temperature in the adhesive remains virtually constant during curing. The thermal history of the adhesive in a joint may be much more different than that in a bulk adhesive specimen. The exothermic reactions during curing provoke a size effect on the temperature. For this reason, during curing of both adhesives, temperature was measured with a thermocouple located at the center of the specimens. The measured temperatures are plotted against time in Fig. 21a for D609 and 21b for E20HP. Maximum temperatures of 80 °C and 27 °C were measured for D609 and E20HP, respectively. A transient analysis in COMSOL Multiphysics finite element software was also performed to evaluate these temperatures by considering a heat source deduced from the DSC results in Fig. 3. The thermal conductivity and heat capacity of the adhesives and the mold were

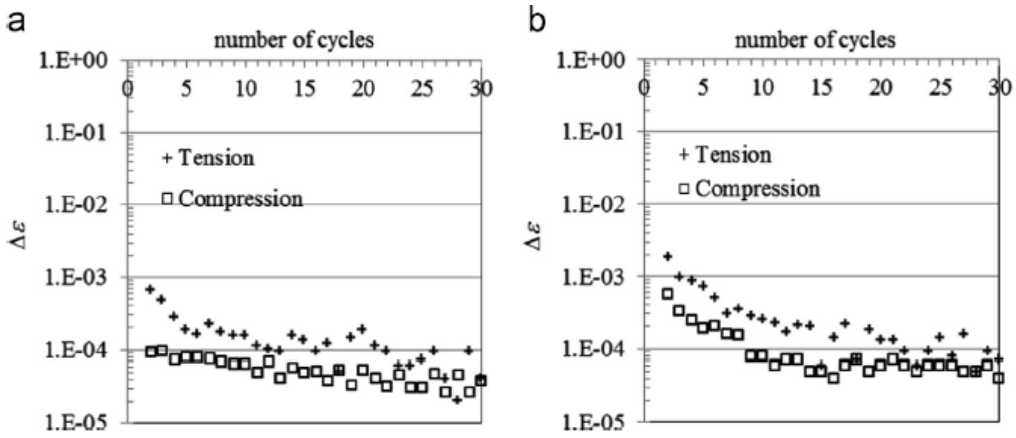

Fig. 17. Ratcheting strains vs number of cycles for D609 (a) and E20HP (b) adhesives in tension and compression.

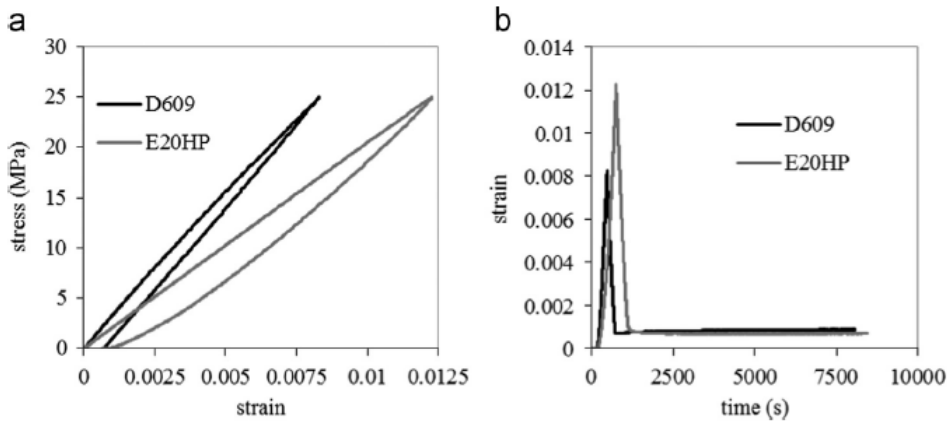

Fig. 18. Stress vs. strain (a) and strain vs. time (b) curves during one-cycle compressive tests.

Considered identical: 0.21 W/ (m K) and 1400 J/(kg K), respectively. The density of the materials was 1150 kg/m3. The predicted temperatures by the finite element calculations are displayed in Fig. 21; these predictions agree satisfactorily with the experimental measurements. The measured temperatures during curing are thus consistent with the heat flow measurements in the DSC.

Since the measured temperature in the E20HP specimens remains reasonably low, the experimental results obtained in this paper for E20HP are relevant to adhesive joints. For the D609 bulk adhesive specimens, the measured temperature is relatively high and similar to the maximum temperature selected for the heat treatment. According to the TGA results in Fig. 2,at 80°C the catalyst and the resin lose less than 0.05% weight; this value seems to be negligible and is likely due to humidity loss. In order to detect an eventual difference between the physical properties of the material in the D609 tensile specimens and those in a very small sample cured at 25 °C, an additional DSC heating scan test was performed with a sample obtained from the center of a bulk adhesive specimen and its heat flow evolution was compared to that showed in Fig. 7 for the 22 mg D609 specimen post-

cured at 70 °C. In Fig. 22, the heat flow for these two samples is plotted against temperature. The two samples provide similar results. Thus, the experimental results obtained in this paper are likely applicable to thin bond lines with a D609 adhesive. A further study, not considered in this paper, is required to confirm this aspect.

As compared to a thin adhesive layer in a joint, bulk adhesive specimens may contain more voids. Few and isolated voids have been observed by trans lucidity in the samples tested in this study. In Fig. 23a, some voids in the volume of a D609 tensile specimen can be observed through its fracture surface which was located at the center of the specimen. The diameter of these voids is less than 0.6 mm. In some fracture surfaces of the specimens tested in

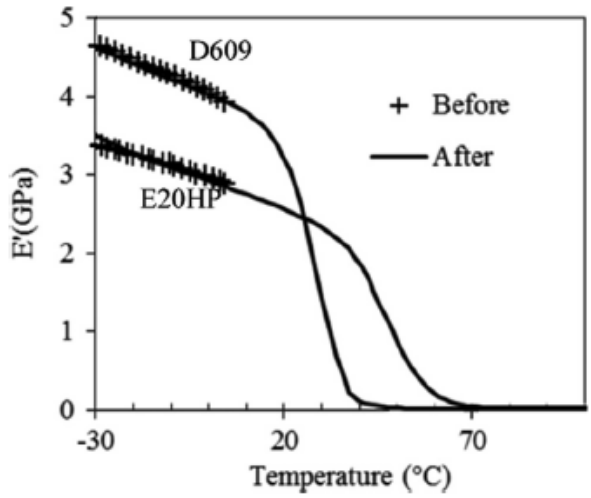

Fig. 19. DMA temperature scanning before and after a temperature exposition for D609 (a) and E20HP (b).

Tension, a void was observed as shown in Fig. 23b. These isolated voids may affect maximum stresses and strains in tension but not the visco-elasto-plastic behavior. Owing to the randomness of void distribution, if this behavior was affected, one or more anomalous curves that would have not verified the observed global

trend would have appeared in Fig. 10 or 12.

4.4. Implications for adhesives behavior models

Whenever one intends to accurately model the behavior of a thermosetting epoxy adhesive, one must start by knowing Tg. If the working temperature is below Tg, the material is in a glassy state and if this temperature is close to Tg a transition to a rubbery

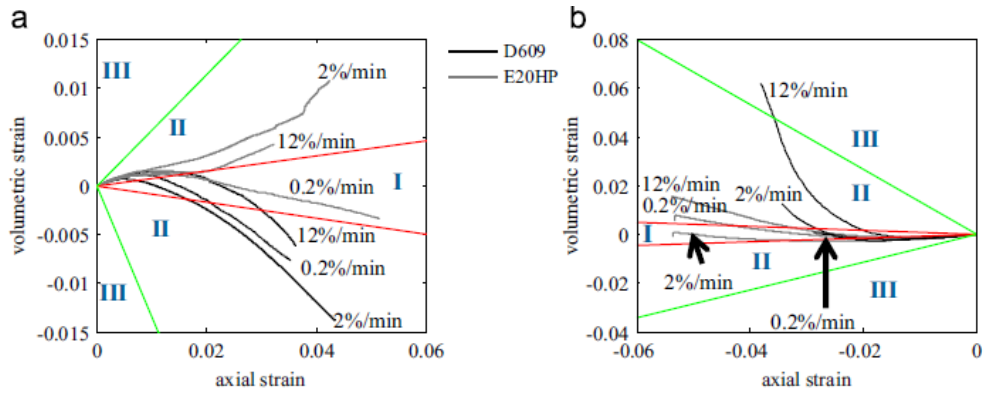

Fig. 20. Uncertainty domains in volumetric vs axial strain plots for monotonic tensile (a) and compressive (b) tests. (For interpretation of the references to color in this figure legend, the reader is referred to the web version of this article.)

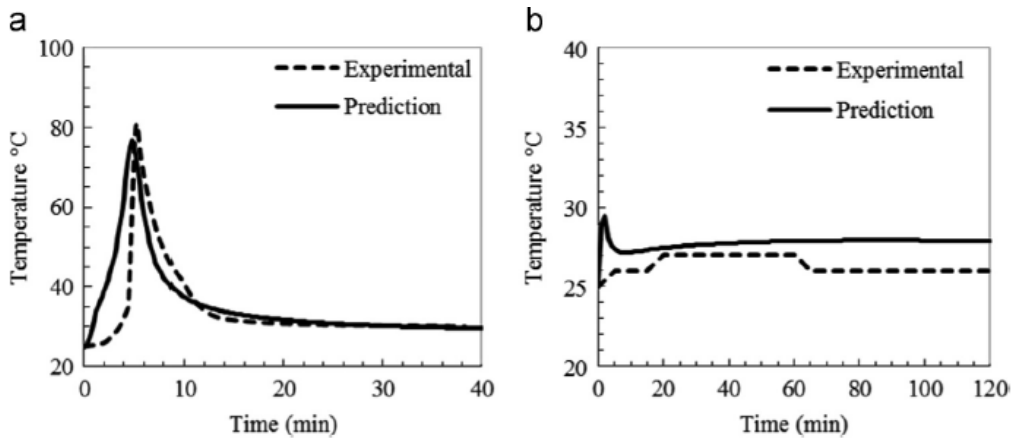

Fig. 21. Temperature during curing of adhesives D609 (a) and E20HP (b), measurements and predictions.

Tate appears. Assuming that we work at a constant temperature below Tg, the model must take into account the following factors:

- The almost constant rate of axial inelastic strains in the creep tests carried out in this work, may suggest the use of a Norton-type flow law [15].
- The inelastic volumetric strains are not negligible with respect to the elastic strains. This phenomenon cannot be modeled using a dissipation potential that involves only the von Mises stress because, in such a case, the inelastic volumetric strains are zero. For example, let us consider a “von Mises material” and adopt an incremental visco-plastic model with isotropic hardening [15]. The following dissipation potential based on a Norton-type flow law is considered:

$$\varphi^* = \frac{K}{n+1}\left\langle \frac{\sigma_{eq} - R - \sigma^c}{K} \right\rangle^{n+1}$$

Where K, n and σc are the material constants; σeq and R are the von Mises stress and the hardening function, respectively. The brackets <x> stand for the positive part of x. assuming a normality rule, the visco-plastic strain rate tensor is deter-mined as follows:

$$\dot{\boldsymbol{\varepsilon}}^{\boldsymbol{p}} = \frac{\partial \varphi^*}{\partial \boldsymbol{\sigma}} = \frac{3}{2}\frac{\boldsymbol{\sigma}^d}{\sigma_{eq}}\dot{p}$$

Where σ, $\sigma^d, \dot{p} = \langle\frac{\sigma eq - R - \sigma^c}{K}\rangle^n$ are the stress tensor, the deviatoric stress tensor and the rate of cumulative plastic strain, respectively. The trace of ε̇p is zero, and thus the visco-plastic volumetric strain is zero. In this way, if one aims at

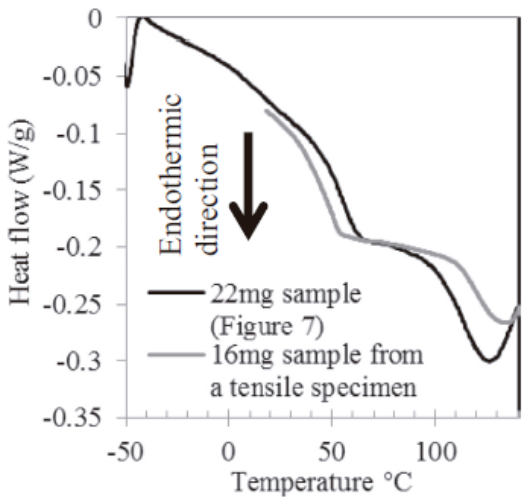

Fig. 22. DSC heating scan of a sample extracted from a tensile specimen and a reference sample (D609 adhesive).

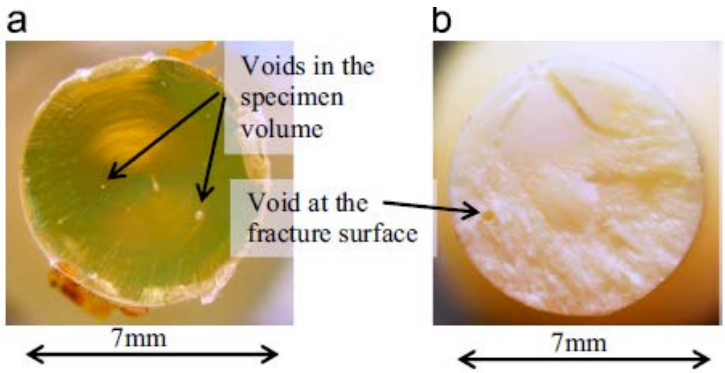

Fig. 23. Fracture surfaces of D609 (a) and E20HP (b) tensile specimens.

Predicting non-zero visco-plastic volumetric strains, the dissipation potential must also involve the hydrostatic stress.

 The modelling of the significant densification in tension and expansion in compression revealed in Sections 3.2 and 3.3, would require a more complex model than a Drucker Prager type one. In a Drucker Prager type model, the equivalent stress in equation (6) is replaced by$\sigma eq + a\sigma h$, where α is a material constant and σh is the hydrostatic stress. Assuming a normality rule ($\dot{\varepsilon}p = \frac{\partial \varphi^*}{\partial \sigma}$), the model would

predict that if $\alpha < 0$, the material would exhibit negative visco-plastic volumetric strains in both tension and compression. On the contrary, if $\alpha > 0$, the material would exhibit positive visco-plastic volumetric strains in both tension and compression. Hence, this model is not able to predict the observed phenomena.

- The cyclic tests revealed a non-negligible ratchetting phenomenon. To reproduce this phenomenon in a behavior model, a kinematic hardening must be incorporated in the model [31].

5. Conclusion

In this work, original visco-elasto-plastic phenomena were revealed in two fast-curing structural epoxy adhesives: D609 and E20HP. First of all, a post-curing process was proposed to ensure a nearly complete curing and achieve stable mechanical properties. Then, the glass transition temperatures were determined. Uniaxial mechanical tests were carried out at 25 °C (below Tg), showing that

- both adhesives have initially a linear elastic behavior independent of the rate and, once the stress exceeds approximately 20 MPa in D609 and 10 MPa in E20HP, there is a visco-elasto-plastic behavior.
- Inelastic volumetric strains are non- negligible and strain rate dependent; they may reach values higher than 20% of the total axial strains and are not a result of small errors in the measurement of strains. This phenomenon cannot be modeled using a dissipation potential that involves only the von Mises stress. In tension, the inelastic volumetric strains can provoke a material densification

(negative volumetric strains). On the contrary, in compression, these inelastic strains cause a material expansion (positive volumetric strains). These phenomena may suggest that “mechanical accelerated aging” and “mechanical rejuvenation” occur at post-yield applied tensile and compressive loads, respectively. A more plausible interpretation is a polyamorphic phase transition [29] accompanied with a specific volume variation,

- after loading the materials above the yield stresses and
- unloading to a zero stress state, non-zero plastic strains were measured, and
- a ratcheting phenomenon appears in cyclic tests.

The measurement of the temperature during curing of the specimens in this paper proved the results obtained with E20HP specimens are relevant to thin bondlines. For D609, the measured temperature reached 80 °C and it is not possible to ensure the applicability of the results to thin bondlines. A further analysis is required for this case.

The results and methods used in this study may be applied to characterize other adhesives. The procedure used to determine the post-curing process can be used for other adhesives that cure at room temperature so as to achieve stable mechanical properties. It is quite possible that other adhesives with Tg’s similar to those ofD609 and E20HP show behaviors similar to those presented in this document at room temperature.

For future works, we consider that it is essential to work on the behavior

modeling of the adhesives considered herein, hoping that the models may be extrapolated to other structural epoxy adhesives. Furthermore, the effect of temperature and physical aging on the adhesives behavior shall be considered.

Acknowledgments

The authors gratefully acknowledge Mónica Elvira Mendoza Duarte, Rubén Castañeda Balderas, Pedro Pizá Ruíz and Daniel Lardizábal Gutiérrez for carrying out the tests exhibited in this paper.

References

[1] Chataigner S, Caron J-F, Duong VA, Diaz Diaz A. Experimental and numerical investigation of shear strain along an elasto-plastic bonded lap joint. Constr Build Mater 2011;25(2):432.

[2] Sampaio EM, Bastian FL, Costa Mattos HS. A simple continuum damage model for adhesively bonded butt joints. Mech Res Commun 2004;31(4):443.

[3] Pap JS, Kästner M, Müller S, Jansen I. Experimental characterization and simulation of the mechanical behavior of an epoxy adhesive. Procedia Mater Sci 2013;2:234.

[4] Wang CH, Chalkley P. Plastic yielding of a film adhesive under multiaxial stresses. Int J Adhes Adhes 2000;20(2):155.

[5] Cognard JY, Badulescu C, Maurice J, Créac'hcadec R, Carrère N, Vedrine P. On modelling the behaviour of a ductile adhesive under low temperatures. Int J Adhes Adhes 2014;48(119).

[6] Goglio L, Peroni L, Peroni M, Rossetto M. High strain-rate compression

and tension behaviour of an epoxy bi-component adhesive. Int J Adhes Adhes 2008;28(7):329.

[7] Cognard JY, Davies P, Sohier L, Créac'hcadec R. A study of the non-linear behaviour of adhesively-bonded composite assemblies. Compos Struct 2006;76(1–2):34.

[8] Drozdov AD. A constitutive model in viscoelastoplasticity of glassy polymers. Polymer 1999;40(13):3711.

[9] Drozdov AD. Viscoelastoplasticity of amorphous glassy polymers. Eur Polym J 2000;36(10):2063.

[10] Drozdov AD. Creep rupture and viscoelastoplasticity of polypropylene. Eng Fract Mech 2010;77(12):2277.

[11] Drozdov AD. Cyclic viscoelastoplasticity and low-cycle fatigue of polymer composites. Int J Solids Struct 2011;48(13):2026.

[12] Mahnken R, Shaban A, Potente H, Wilke L. Thermoviscoplastic modelling of asymmetric effects for polymers at large strains. Int J Solids Struct 2008;45 (17):4615.

[13] Chaboche JL. Thermodynamic formulation of constitutive equations and application to the viscoplasticity and viscoelasticity of metals and polymers. Int J Solids Struct 1997;34(18):2239.

[14] Poulain X, Benzerga AA, Goldberg RK. Finite-strain elasto-viscoplastic behavior of an epoxy resin: experiments and modeling in the glassy regime. Int J Plast 2014;62:138.

[15] Lemaitre J, Chaboche JL. Mechanics of solid materials. Cambridge:

Cambridge University Press; 1990.

[16] Merrall GT, Meeks AC. Effect of thermal aging on mechanical properties of an epoxy resin system. J Appl Polym Sci 1972;16(12):3389.

[17] Jiang H, Wang R, Farhan S, Zheng S. Properties and curing behavior of reactive blended allyl novolak with bismaleimide using dicumyl peroxide as a novel curing agent. J Appl Polym Sci 2015;132:15.

[18] Santana IL, Lodovici E, Matos JR, Medeiros IS, Miyazaki CL, Rodrigues-Filho LE. Braz Dent J 2009; 20(3):205.

[19] Moussa O, Vassilopoulos AP, de Castro J, Keller T. Time–temperature dependence of thermomechanical recovery of cold-curing structural adhesives. Int J Adhes Adhes 2012; 35:94.

[20] Al-Safy R, Al-Mahaidi R, Simon. GP. A study of the practicality and perfor-mance of CFRP applications using post-curing at moderately elevated tem-peratures. Compos Part B – Eng 2013; 48:140.

[21] Ferracane JL, Condon JR. Post-cure heat treatments for composites: properties and fractography. Dent Mater 1992;8(5):290.

[22] Cognard JY, Davies P, Gineste B, Sohier L. Development of an improved adhesive test method for composite assembly design. Compos Sci Technol 2005;65(3–4):359.

[23] Odegard GM, Bandyopadhyay A. Physical aging of epoxy polymers and their composites. J Polym Sci Polym Phys 2011;49(24):1695.

[24] Elkoun S, G'Sell C, Cangemi L, Meimon Y. Characterization of volume strain of poly(vinylidene fluoride) under creep test. J Polym Sci Polym Phys 2002;40

(16):1754.

[25] Cangemi L, Elkoun S, G'Sell C, Meimon Y. Volume strain changes of plasticized poly(vinylidene fluoride) during tensile and creep tests. J Appl Polym Sci 2004;91(3):1784.

[26] Colucci DM, O'Connell PA, McKenna GB. Stress relaxation experiments in polycarbonate: a comparison of volume changes for two commercial grades. Polym Eng Sci 1997;37(9):1469.

[27] Myers FA, Cama FC, Sternstein SS. Mechanically enhanced aging of glassy polymers. Ann NY Acad Sci 1976;279:94.

[28] Oyanguren PA, Vallo CI, Frontini PM, Williams RJ. Rejuvenation of epoxy glasses subjected to uniaxial compression. Polymer 1994;35(24):5279.

[29] McKenna GB. Mechanical rejuvenation in polymer glasses: fact or fallacy? J Phys – Condens Mater 2003;15(11):S737.

[30] Lacks DJ, Osborne MJ. Energy landscape picture of overaging and rejuvenation in a sheared glass. Phys Rev Lett 2004;93(25):255501.

[31] Halama R, Sedlák J, Šofer M. Phenomenological modelling of cyclic plasticity. In: Miidla P, editor. Numerical modelling. InTech. p. 329–54. Available from: /http://www.intechopen.com/books/numerical-modelling/phenomen ological-modelling-of-cyclic-plasticityS; 2012. ISBN: 978-953-51-0219-9.